

# Mechanical and tribological behavior of flyash, red mud and mica particles reinforced Al7075 alloy hybrid metal composites

Siddesh Matti<sup>1</sup>, B.P. Shivakumar<sup>1</sup>, Madeva Nagaral<sup>2</sup> , S. Shashidhar<sup>3</sup>, P.N. Siddappa<sup>1</sup>, and Virupaxi Auradi<sup>4</sup> 

<sup>1</sup> Department of Mechanical Engineering, JSS Academy of Technical Education, Bangalore, Karnataka, India

<sup>2</sup> Aircraft Research and Design Centre, HAL, Bangalore, Karnataka, India

<sup>3</sup> Department of Mechanical Engineering, UVCE, Bangalore, Karnataka, India

<sup>4</sup> Department of Mechanical Engineering, Siddaganga Institute of Technology, Tumakuru, Karnataka, India

Received: 16 January 2022 / Accepted: 4 April 2022

**Abstract.** In the present research Al7075 alloy with 1, 3 and 5 varying weight percentages of flyash, 1, 2 and 3 varying wt.% of red mud along with constant 4 wt.% of mica particles composites were synthesized by stir casting technique. Thus prepared Al7075 alloy composites were subjected to the microstructural characterization using SEM and EDS. Mechanical properties were evaluated to know the impact of multi micro particles addition on the hardness, ultimate strength, yield strength, and ductility behavior of Al7075 alloy composites. Further, wear behavior of the prepared Al7075 alloy with mica, flyash and redmud composites were experimented using pin-on-disc apparatus by varying normal load and sliding velocity at constant 3000 m sliding distance. The improved mechanical properties were observed with the addition of micro scaled flyash, redmud and mica particles, further improvement was attained with the increasing weight percentage of flyash and red mud in the Al7075 matrix alloy. However, there was decrease in the ductility of the composites with an incorporation of hard micro particles in the soft Al matrix. Fractography and worn surface analysis were carried out to know the influence of micro particles on the tensile failure and wear surfaces of the composites.

**Keywords:** Al7075 alloy / fly ash / red mud / mica / hardness / tensile strength / fractography / wear

## 1 Introduction

Due to their enriched properties such as high strength and lightweight, low thermal conductivity, wear resistance, and high operating temperature, aluminium metal matrix composites (AMMCs) have gained worldwide attention in the field of research in military applications to manufacture armour tanks, bullet proof jackets, automobile body parts, aeronautical applications, space, and the automotive industries [1,2]. Due to their higher strength, heat treatable aluminium alloys such as Al2021, Al6061, and Al7075 are often used, and metal matrix composites (MMCs) manufactured with these alloys have improved thermal stability [3,4]. The qualities of AMMCs can be improved by choosing the right reinforcing geometry, type, and form, as well as the right fabrication technique [5].

The addition of tougher and higher-strength ceramic particles to a metal matrix with medium strength, and low stiffness can improve qualities that are intermediate between the ceramic and the base matrix [6]. The qualities

of MMCs are largely determined by the processing method used. The processing approaches for manufacturing composites are determined by whether the reinforcement is added to the matrix in a solid or liquid state [7,8]. Stir casting is a favoured processing technique for fabricating composites in the liquid state because of its flexibility, economy, and ability to generate bulk quality production [9]. The liquid state technique works on the premise of melting the matrix material, then adding reinforcement to the melt to get the desired dispersion.

Because of various advanced properties particles reinforced MMCs can be successfully used as cutting tools in high speed finishing and cutting applications in the current era [10,11]. This developed interest in research to use attractive combinations of flyash, red mud and mica as reinforcement and study the effect of its addition on properties of Al7075 alloy. These prepared composites were characterized by microstructure studies using SEM/EDX.

Al-7Si-fly ash composites have been attempted to be synthesised and evaluated for their mechanical characteristics by Nagaraj et al. [12]. Vortex processing was used to create fly ash-reinforced Al-7Si alloy composites. The quantity of fly ash was adjusted in steps of 3, that is,

\* e-mail: [madev.nagaral@gmail.com](mailto:madev.nagaral@gmail.com)

**Table 1.** Chemistry of Al7075 alloy.

Element	Cu	Cr	Mn	Mg	Si	Ti	Zn	Fe	Al
Wt. %	1.8	0.2	0.4	1.9	0.5	0.15	3.25	0.5	Balance

between 3% and 6% of fly ash in the Al-7Si alloy, respectively. Preheated fly ash particles were used to create all of the composite materials used in this study. The microstructures of cast Al-7Si, Al-7Si-3wt.% fly ash, and Al-7Si-6wt.% fly ash were examined using optical and SEM and EDS, respectively, to determine their composition. Furthermore, the mechanical properties of the produced samples were examined in accordance with ASTM standards, including hardness, ultimate and yield strength. The Al-7Si alloy matrix was shown to have a homogeneous distribution of fly ash based on microstructural investigation. The Al-7Si matrix was found to contain fly ash during an EDS study. In comparison to the Al-7Si base alloy, Al-7Si-fly ash composites showed better hardness and enhanced tensile characteristics. It's an Al-7Si alloy combined with 3 to 6 wt.% fly ash composites were effectively prepared using the liquid metallurgical process. The homogeneous distribution of fly ash particles in the Al-7Si alloy matrix was demonstrated by microstructural experiments using optical and scanning micro photography. The fly ash in Al-7Si-fly ash composites was discovered using an EDS assay. The Al-7Si-fly ash composite was shown to have a harder than the basal Al matrix. The addition of 6 wt.% of fly ash particles increased the UTS of the Al-7Si matrix system by 19.5%. The Al-7Si-3 and 6 wt.% fly ash composites were shown to have higher yield strength than the basal matrix. After adding 6 wt.% of fly ash particles to the basic matrix Al-7Si, the yield strength rose from 143 MPa to 169 MPa.

Individual and multiple particle reinforcements on AMMCs, such as Hybrid MMC, are finding growing usage in aerospace, vehicle, space, submarine, and transportation applications by Saravanan et al. [13]. Improved mechanical and tribological qualities such as strength, stiffness, abrasion resistance, impact resistance, and wear resistance are the key reasons for this. A lot of research initiatives were on the pipeline in the current circumstance. This study directs researchers and engineers to the right selection of materials in the relevant field based on their qualities, as well as the many procedures used in the fabrication of MMC, with a focus on the liquid state metal processing approach. Aluminium alloys are the chosen engineering material for numerous high-performing components that are utilised for a variety of applications in the car, aircraft, and mineral processing sectors, due to their reduced weight and good thermal conductivity features. Heat treatable Al6061 and Al7075 are two series of aluminium alloys that have been extensively studied. Al6061 alloy is extremely corrosion resistant, has moderate strength, and is widely used in construction, automotive, and marine applications. Aluminum alloy 7075 is used in the aerospace and car industries because of its great strength and durability. Composites made of aluminium

alloys are popular because of their high strength, wear resistance, and stiffness. Furthermore, when supplemented with ceramic particles, these composites are superior in nature for high-temperature applications.

In this work, Al7075 alloy hybrid composites were set up by keeping 4 wt.% of mica constant with 1, 3, 5 varying wt.% of flyash and 1, 2, 3 varying wt.% of red mud particles in the Al7075 alloy. Thus prepared composites were evaluated for various mechanical and tribological properties as per ASTM methods.

## 2 Experimental details

### 2.1 Material used

#### 2.1.1 Al7075 alloy

The Al7075 compound was chosen as the framework material due to its unique features and vast range of uses in today's world. The Al7075 compound configuration is shown in Table 1.

#### 2.1.2 Reinforcement materials

Flyash, red mud and mica particles are used as hybrid reinforcements in Al7075 matrix material. The average particle size of mica, flyash and red mud used in the study are 10 microns. As shown in Figure 1, mica, fly ash, and red mud with particle sizes of 10  $\mu\text{m}$  were utilized as reinforcements in the manufacture of MMCs (a-c). Table 2 is showing the chemical composition of mica particles and Tables 3 and 4 are indicating chemical composition of flyash and red mud respectively.

### 2.2 Composite preparation and testing

Hybrid composites with varied degrees of hybrid reinforcements were created using the liquid metallurgy approach. At 760°C, aluminium 7075 alloy was melted in an electrical resistance furnace. With the use of a mechanical stirrer, a vortex was generated in liquid aluminium and blended. Pre-mixed powders of fly ash, red mud, and mica were gradually added to the vortex as it was mixing. Mica, fly ash, and red mud were heated for one hour in a heater before being blended at 200°C. Spraying lubrication into the mould cavity was used to equip the metallic dies. To manage the temperature and assist the simple evacuation of the material, oil was splashed over the bite the dust. Microstructure investigations, hardness, tensile, and wear tests were performed on the cast Al7075 and its hybrid composites, which were machined to standard specifications. An automated metallurgical magnifying lens was used to examine the microstructure of metallographically cleaned cast combination and mixture composites.

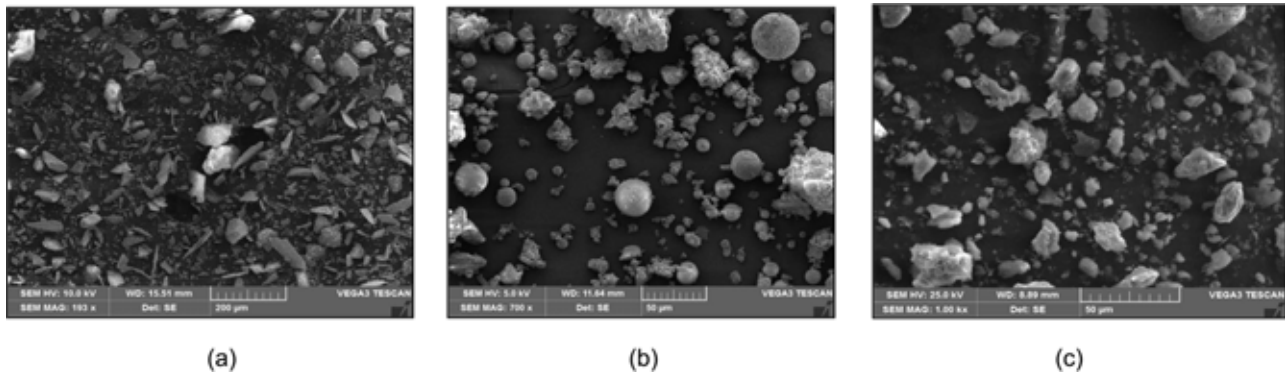


**Fig. 1.** SEM graphs of (a) mica, (b) fly ash, (c) red mud particles.

**Table 2.** Chemistry of mica particles.

Compounds	Weight percentage
Silica ( $\text{SiO}_2$ )	45.57
Alumina ( $\text{Al}_2\text{O}_3$ )	33.10
Potassium Oxide ( $\text{K}_2\text{O}$ )	9.87
Ferric Oxide ( $\text{Fe}_2\text{O}_3$ )	2.48
Sodium Oxide ( $\text{Na}_2\text{O}$ )	0.62
Titanium Oxide ( $\text{TiO}_2$ )	Traces
Calcium Oxide ( $\text{CaO}$ )	0.21
Magnesia ( $\text{MgO}$ )	0.38
Moisture at 100 °C	0.25
Phosphorus (P)	0.03
Sulphur (S)	0.01
Graphite Carbon (C)	0.44
Loss on Ignition ( $\text{H}_2\text{O}$ )	2.74

**Table 3.** Chemistry of flyash particles.

Compounds	Weight percentage
$\text{SiO}_2$	52
$\text{Al}_2\text{O}_3$	26
$\text{Fe}_2\text{O}_3$	5
$\text{CaO}$ (Lime)	10
$\text{MgO}$	4
$\text{SO}_3$	3

**Table 4.** Chemistry of red mud particles.

Compounds	Weight percentage
$\text{Fe}_2\text{O}_3$	55
$\text{Al}_2\text{O}_3$	15
$\text{SiO}_2$	20
$\text{Na}_2\text{O}$	6
$\text{CaO}$	3.75
$\text{TiO}_2$	trace-0.25

The model is now available for microstructural inspection with a scanning microscope to determine the even distribution of particles in the Al7075 composite after projection. Al7075 alloy and Al7075 composites containing mica, fly ash, and red mud particles are microstructured. The microstructure is estimated to measure 15 mm broad and 5 mm tall, according to the model. The model's surface is refined with papers with coarseness's of 300, 600, and 1000. After that, the surface is cleaned with cleaning paper to give the cleaning machine an additional smooth finish. The models are then cleaned with refined water to eliminate any additional particles, such as dust and other contaminations, that may have accumulated on the cleansed surface. To achieve a distinguishing surface, Keller's reagent [14] is used to scratch the models.

The model is also machined for hardness testing, according to ASTM E10. To determine hardness, a Brinell hardness analyzer equipment is employed. The surface of the model has been cleaned and smoothed. The tensile models are machined according to ASTM standard E8 [15]. As illustrated in Figure 2, the model's overall length is 104 mm, the measure length is 45 mm, and the gauge dia. is 9 mm. This tensile test is used to estimate the percentage elongation of Al7075 alloy and its composites. A pin-on-disc wear apparatus was used to conduct wear and friction testing in accordance with ASTM G99 [16]. The wear test specimens utilised in the investigation are shown in Figure 3. Wear specimen are machined as per ASTM G 99 standard with 8 mm in diameter and 300 mm in length. Wear tests are conducted at 30 N load, 500 rpm sliding speed and with 3000 m sliding distance.

## 3 Results and discussion

### 3.1 Microstructural studies

SEM with EDS attachment is used to examine the microstructural characterizations of specimens. SEM micrographs of Al7075 material with mica, flyash, and red mud micro particles reinforced composites without heat treatment are shown in Figures 4a–c. The SEM of pure Al7075 alloy is shown in Figure 4a. SEM images of Al7075 alloy with constant 4 wt.% mica, 3 wt.% flyash, and 3 wt.% red mud particles reinforced hybrid composites and Al7075 alloy with constant 4 wt.% mica, 5 wt.% flyash, and 3 wt.%



**Fig. 2.** Tensile test specimen.



**Fig. 3.** Wear test specimen.

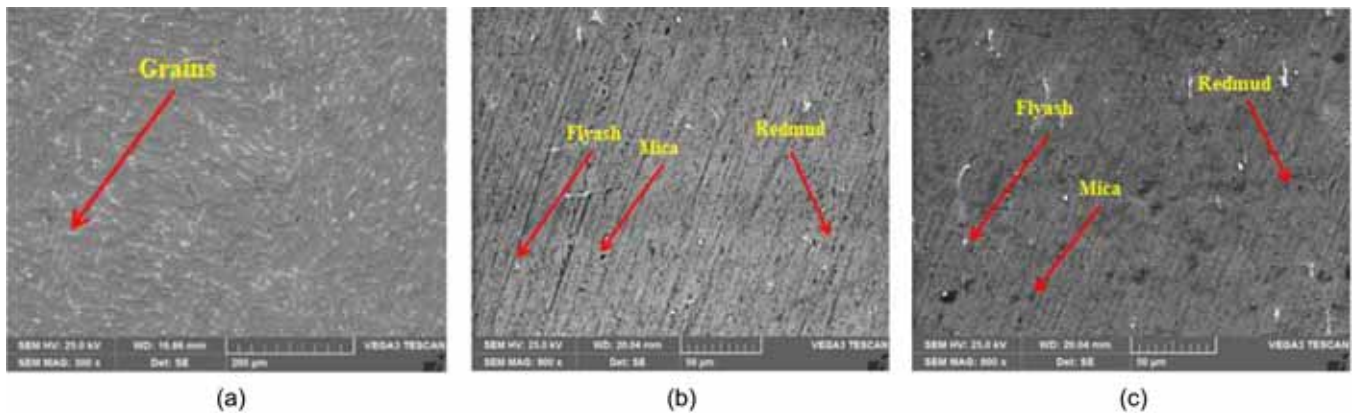


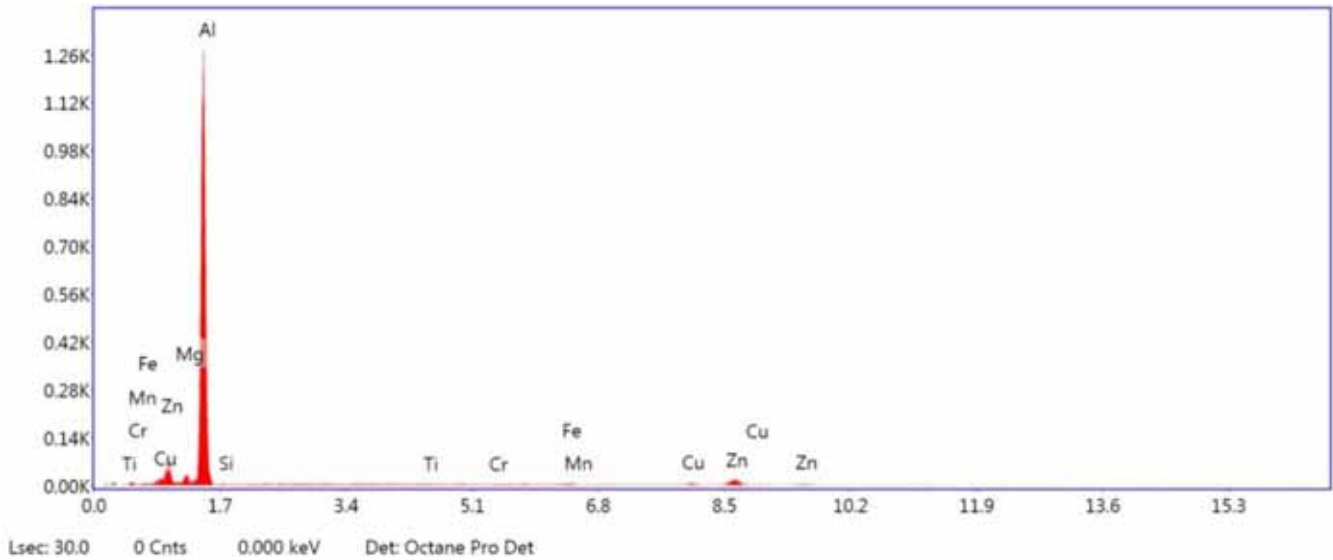
**Fig. 4.** SEM micrographs of (a) Al7075 alloy, (b) Al7075-4% Mica – 3% fly ash-3% Red mud, (c) Al7075-4% Mica – 5% fly ash-3% Red mud composites.

red mud reinforced hybrid composites are shown in Figures 4b–c. As an unreinforced alloy, the SEM micrograph of as cast Al7075 alloy is free of particles. The Al7075 alloy is a heat treatable alloy since it contains Zn as the main alloying element. In addition, Figures 4b–c shows that the mica, flyash, and red mud particles in the produced hybrid composites are homogeneous. The Al7075 alloy composites' enhanced reinforcing content is also visible in the microphotographs. As can be seen in Figure 4c, adding 4 wt.% mica micro, 5 wt.% flyash, and 3 wt.% red mud particles to the Al7075 matrix in two stages improved the microstructure of the composite significantly.

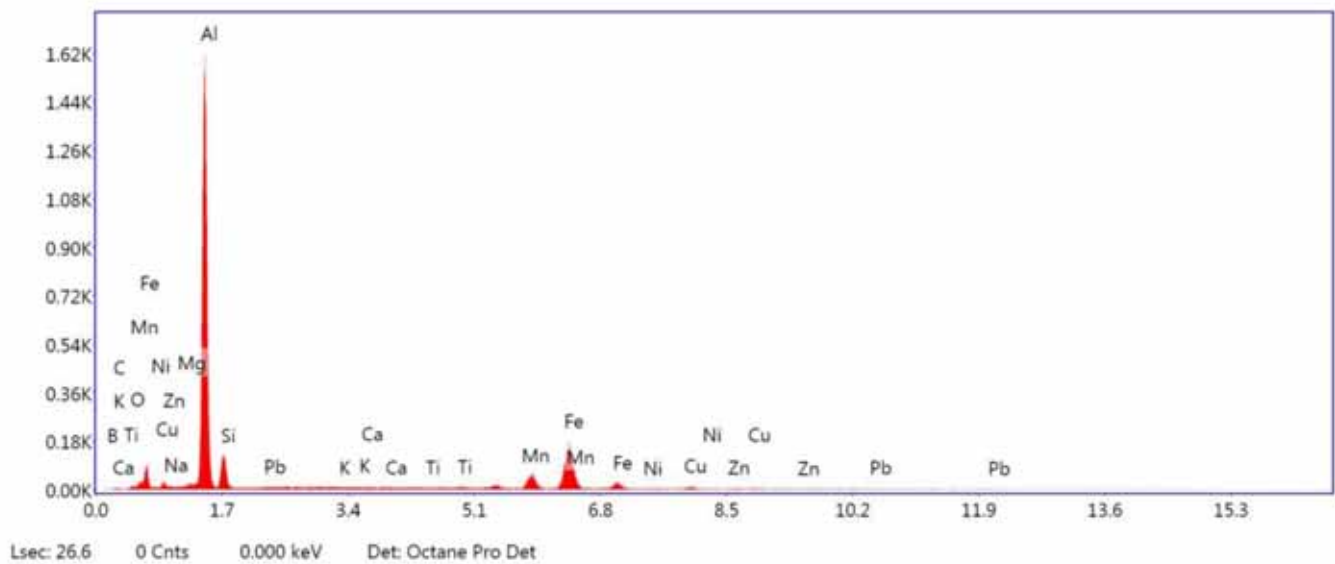
Figure 5a indicates the EDS spectrum of Al7075 alloy which confirmed the main alloying components like Si, Fe, Cu, Mn, Zn, Cr, and Ti in the Al matrix. Figure 5b representing the elemental analysis of Al7075 with 4 wt.%

of mica and 5 wt.% of flyash and 3 wt.% of red mud hybrid composites. In both tri particulates reinforced hybrid composites, the presence of micro mica, flyash and red mud particulates confirmed by various elements as shown in the EDS spectrum. The presence of mica in the Al7075 alloy is confirmed by all the relevant elements. Usually, mica particulates contain  $\text{SiO}_2$  phase, this  $\text{SiO}_2$  phase is confirmed by the elements like Si and O shown in Figure 5b. Similarly, other phases of CaO, C, MgO,  $\text{K}_2\text{O}$ ,  $\text{Fe}_2\text{O}_3$ ,  $\text{Al}_2\text{O}_3$  and  $\text{Na}_2\text{O}$  are present in the mica, flyash and red mud particulates are confirmed by elements like Ca, O, C, Mg, K, Fe, Al and Na in the energy dispersive spectrographs as shown in Figure 5b.

Figures 6a–b shows the XRD pattern taken for as cast aluminium alloy Al7075 alloy and Al7075 alloy with 4 wt.% of mica, 5 wt.% of flyash and 3 wt.% of micro red mud



(a)



(b)

**Fig. 5.** (a–b) EDS graphs of (a) Al7075 alloy (b) Al7075 alloy-4% mica-5% flyash and 3% red mud hybrid composites.

composites without heat treatment process to verify its quality and standard XRD pattern respectively. It may be seen that peak increments and afterward diminishes on 2-theta scale demonstrating the presence of various periods of material. In Figure 6a it is noticeable that X-ray beam forces of pinnacle are higher at 38, 45° and 65° demonstrating the presence of aluminum compound. Figure 6b shows the XRD pattern taken for mica, flyash and red mud Al7075 alloy composites to verify its quality and standard XRD pattern. It is observed the peaks for different phases of aluminium, mica, flyash and red mud compositions at various phases' present hybrid composites.

### 3.2 Hardness measurements

Table 5 and Figure 7 shows the comparison between hardness of Al7075 with varying weight percentages of fly ash and red mud particles with constant 4 wt.% of mica particles reinforced hybrid composites.

The hardness of Al7075 alloy as cast and Al7075 alloy with constant 4 wt.% mica, 1, 3, 5 varying weight percentages of flyash, and 1, 2 and 3 varied weight percentages of red mud particles reinforced hybrid composites are shown in Figure 7 and Table 1. The plot shows that the hardness of the Al7075 alloy increases with a constant 4 wt.% of mica and increasing wt.% of flyash and

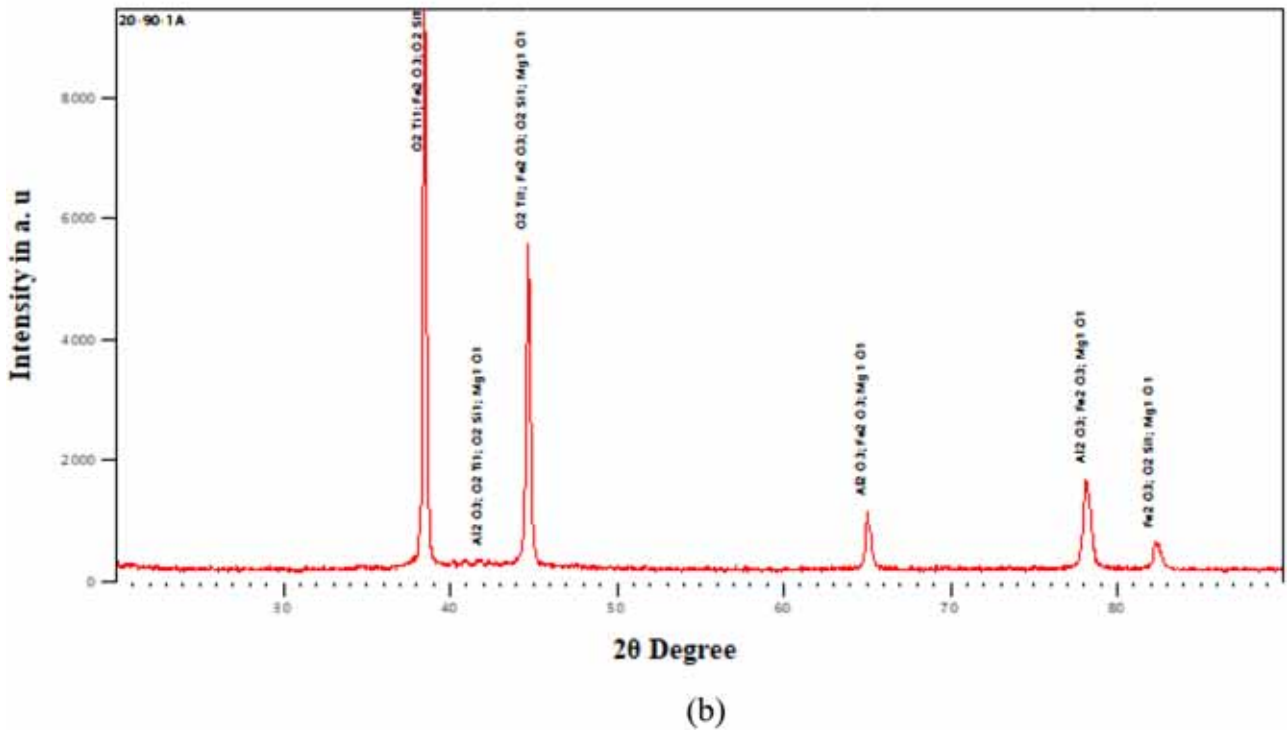
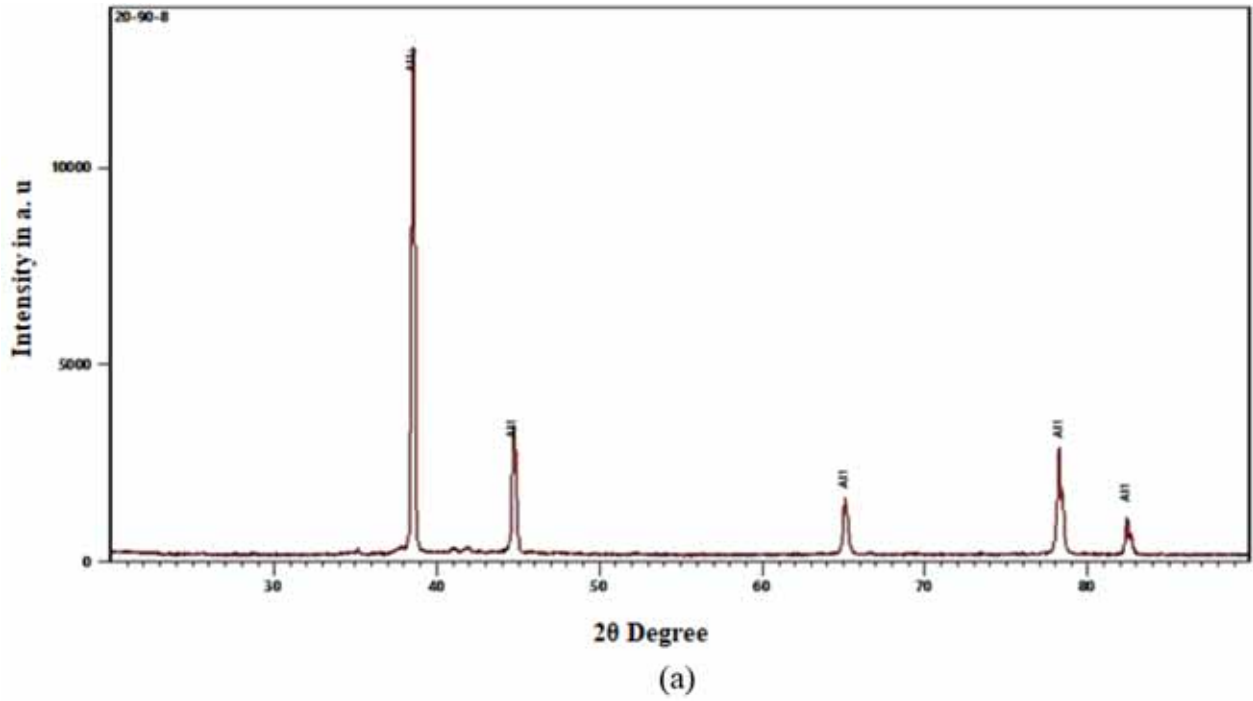


Fig. 6. (a-b) XRD patterns of (a) Al7075 alloy (b) Al7075 alloy-4% mica-5% flyash and 3% red mud particles hybrid composites.

**Table 5.** Comparison of hardness of Al7075 with 4 wt.% of constant mica, varying wt.% of flyash and red mud composites.

Sl. No	Composition	Hardness (BHN)
1	Al7075 Alloy	56.4
2	Al7075 with 4% Mica, 1% Flyash and 1% Red Mud	74.2
3	Al7075 with 4% Mica, 3% Flyash and 1% Red Mud	75.3
4	Al7075 with 4% Mica, 5% Flyash and 1% Red Mud	78.9
5	Al7075 with 4% Mica, 1% Flyash and 2% Red Mud	75.2
6	Al7075 with 4% Mica, 3% Flyash and 2% Red Mud	81.2
7	Al7075 with 4% Mica, 5% Flyash and 2% Red Mud	84.3
8	Al7075 with 4% Mica, 1% Flyash and 3% Red Mud	77.2
9	Al7075 with 4% Mica, 3% Flyash and 3% Red Mud	86.2
10	Al7075 with 4% Mica, 5% Flyash and 3% Red Mud	88.1

red mud particles in the Al7075. The BHN of Al7075 alloy as cast is 56.4 BHN. The hardness of Al7075 alloy is also improved by the inclusion of varied flyash and red mud particles, as well as a constant 4 wt.% of mica. The Al7075 alloy reinforced composites containing 4 wt.% mica, 5 wt.% flyash, and 3 wt.% red mud particles had the maximum hardness, with an 88.1 BHN. The addition of these tri particles to the Al7075 alloy improves the hardness by 56.2%. The inclusion of tri particles in the Al matrix improves the hardness of Al7075 alloy. These flyash, mica, and red mud particles operate as a surface deformation barrier when a load is applied to it [17]. The good interfacial bonding between the mica, flyash and redmud particles with Al7075 alloy helped in improving the hardness.

### 3.3 Tensile properties

Figures 8 and 9 showing the ultimate and yield strength of Al7075 alloy its mica, flyash and red mud hybrid composites respectively. The strength of as cast Al7075 alloy is 181.8 MPa and 137.9 MPa. Further, with the addition of constant 4 wt.% of mica, varying wt.% of flyash (1, 3 and 5) and varying wt.% of red mud (1, 2 and 3) there is increase in UTS and YS of Al7075 alloy. The highest ultimate and yield strengths are obtained in the Al7075 alloy reinforced with 4 wt.% of mica, 5 wt.% of flyash and 3 wt.% of red mud particles composites. The ultimate and yield strength in these composites are 302.6 MPa

and 213.6 MPa respectively. The improvements obtained in UTS and YS with the addition of these particles are 66.4% and 54%. The increased strength achieved by including these particles is mostly owing to the high strength of the particles, which function as barriers to plastic deformation. Preheating of reinforcing particles improves interfacial strength and allows for high diffusion of reinforcing particles during the composite construction process [18]. Due to the existence of hard phase, which works as resistance to plastic deformation, the reinforcement in addition to the matrix withstands the total load during the use of external load on the composite. During solidification, the difference in average coefficients of thermal expansion between matrix ( $23.2 \times 10^{-6}/C$ ) and reinforcement ( $7 \times 10^{-6}/C$ ) causes a high density of dislocations to form around all of these tri particles. The strength of the contact between dislocations and particles is improved [19].

The elongation of Al7075 compound with various wt.% of flyash and red mud and a fixed weight level of mica is shown in Figure 10. The effect of mica, fly ash, and red mud expanding on the Al7075 amalgam's flexibility is shown. The malleability of Al7075 compound is reduced when hard particles are present. The rate extension achieved in the as cast Al7075 composite with 4 wt.% mica, 1 wt.% fly ash, and 1 wt.% red mud was 13.1 percent. Furthermore, increasing the weight percent of flyash particles from 1 to 5 wt.%, together with consistent 4 wt.% mica and 1 to 3 wt.

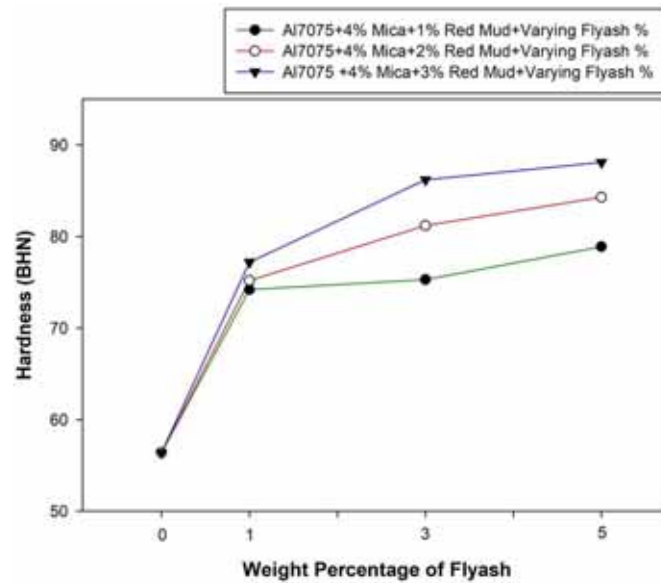


Fig. 7. Hardness of Al7075 with constant 4 wt.% of mica and varying wt.% of flyash and red mud hybrid composites.

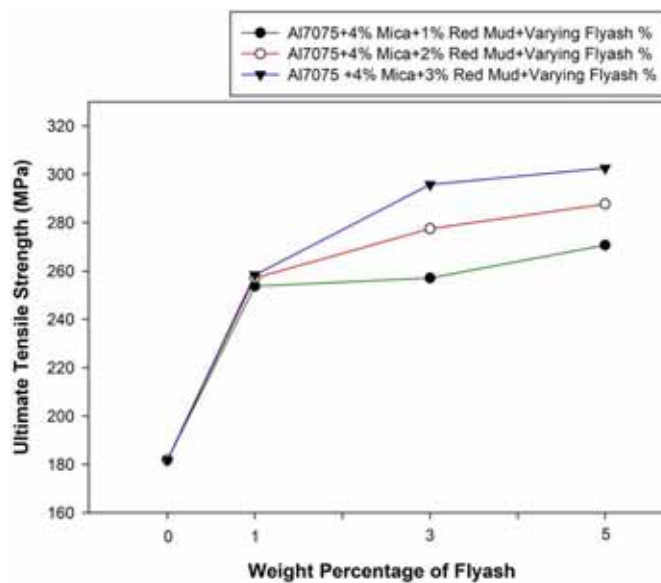


Fig. 8. UTS of Al7075 with constant 4 wt.% of mica and varying wt.% of flyash and red mud hybrid composites.

% red mud, reduces the Al7075 composite's longevity. Hybrid composites including 4 wt.% mica, 5 wt.% flyash, and 3 wt.% red mud reinforced composites with 10.92% had the lowest ductility. The decrease in stretching is mostly due to the weakening of the sensitive framework due to the consolidation of hard particles. The pliability of ceramics decreases due to their poor conductivity.

### 3.4 Tensile fractography

The size and concentration of reinforcement, as well as the processing circumstances, all play a role in composite fracture. Particle debonding, matrix failure, and particle

fracture are the most common causes of failure in aluminium composites. SEM fracture study of Al7075 composites was performed and the results are shown in Figures 11a–c. Figure 11a indicating the tensile fracture behavior of as-cast Al7075 alloy, which is showing grains with more plastic deformation and larger cavities and grooves on the fractured surfaces. Figure 11b shows the tensile fractured surface of Al7075 with 4 wt.% mica-3 wt.% fly ash and 3 wt.% red mud hybrid composites, while Figure 11c shows the tensile fractured surface of Al7075 alloy with 4 wt.% mica-5 wt.% fly ash and 3 wt.% red mud hybrid composites. The tensile behavior of Al7075 alloy was affected by the addition of mica particles. In this study,

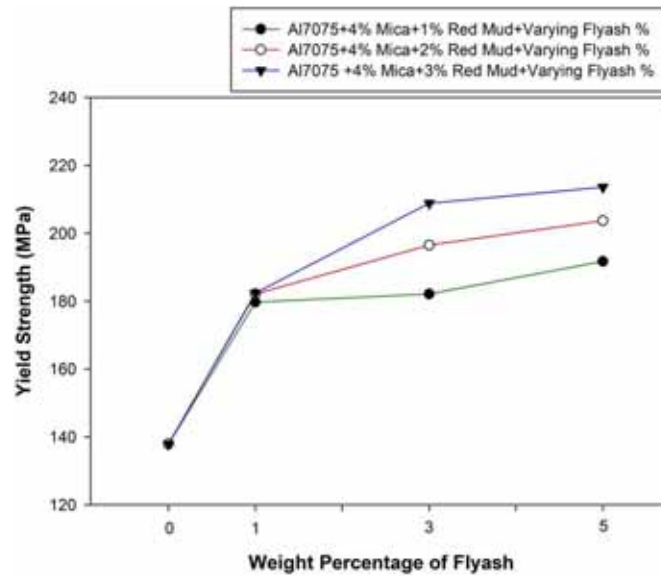


Fig. 9. YS of Al7075 with constant 4 wt.% of mica and varying wt.% of flyash and red mud particles composites.

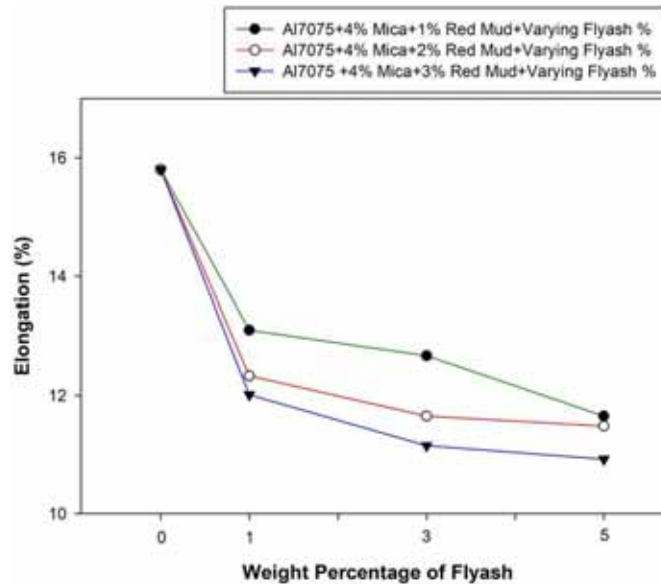


Fig. 10. Ductility of Al7075 with constant 4 wt.% of mica and varying wt.% of flyash and red mud particles hybrid composites.

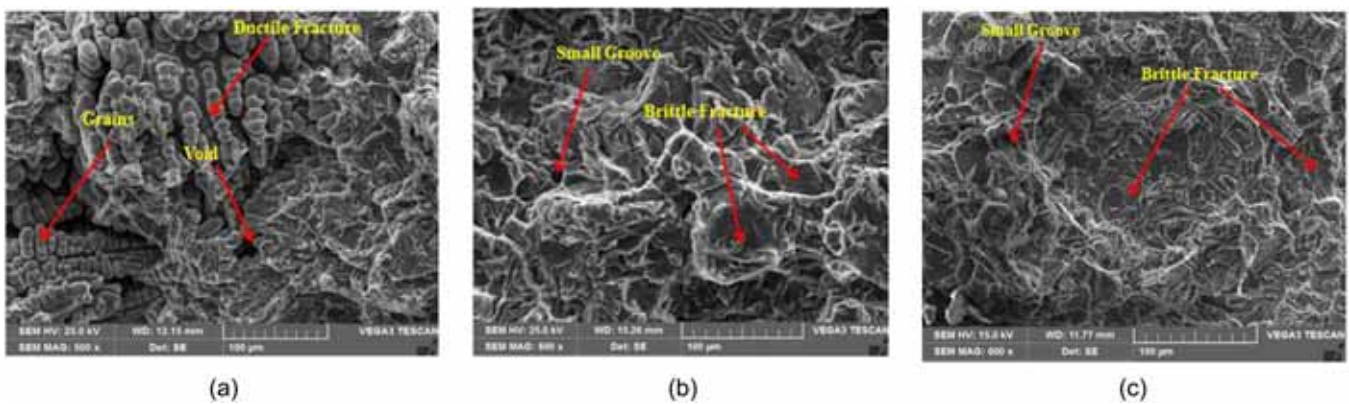


Fig. 11. Tensile fracture surfaces of (a) As cast Al7075 alloy (b) Al7075-4% Mica - 3% fly ash-3% Red mud (c) Al7075-4% Mica- 5% fly ash-3% Red mud composites.

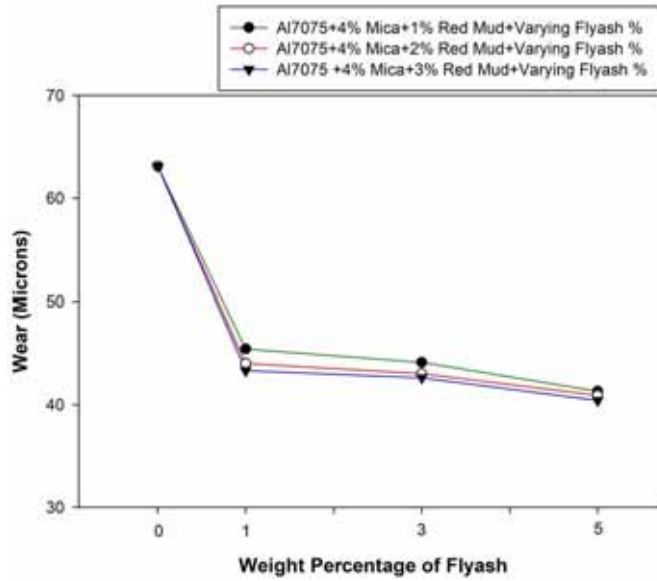


Fig. 12. Wear behavior of Al7075 alloy and its mica, flyash and red mud particles reinforced hybrid composites.

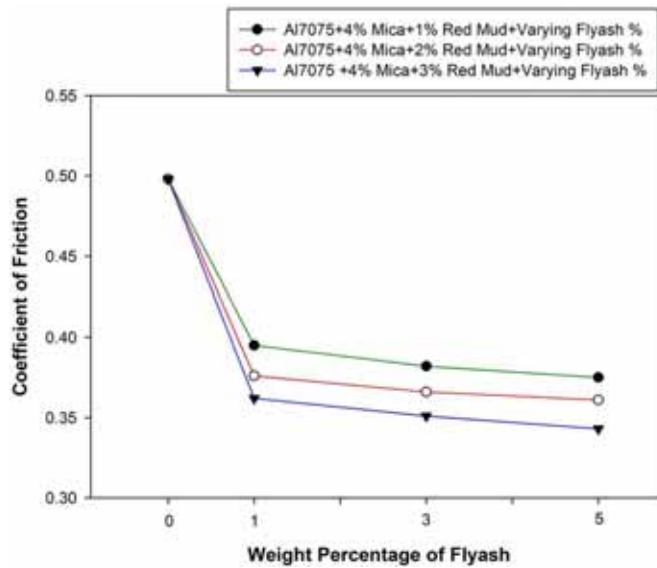


Fig. 13. Co-efficient of friction of Al7075 alloy and its mica, flyash and red mud particles reinforced hybrid composites.

the wt.% of flyash particles increased from 1 to 3 wt.%, and the weight percentage of red mud particles varied from 1 to 3 wt.%. As these particles content improved, the Al7075 alloy exhibited brittle fracture.

The composites display a mix of brittle and ductile failure modes as they approach failure. The microvoids are shown to be nucleated at the interdendritic areas, followed by coalescence. Reinforcement particles and their tiny clusters were discovered in some of these microvoids. It's possible that these clusters represent nucleation locations for composite rupture, hastening composite failure in a brittle manner. When particles have a strong bond with the matrix, particle cracking is a significant potential. By breaking particles, high stress concentrations induced by a

large number of dislocations will nucleate cracks [20]. As a result, the elongation of composites is slightly lower than that of the unreinforced alloy.

### 3.5 Wear and friction

The wear and friction behaviour of as cast alloy and changing flyash and red mud particles with constant mica particles reinforced hybrid composites is shown in Figures 12 and 13. The graphs show that as the weight percentage of fly ash increases from 1 to 5 wt% and the content of red mud particles increases from 1 to 3 wt%, wear loss decreases as compared to the based matrix. Also, the figures show that when the weight % of these particles

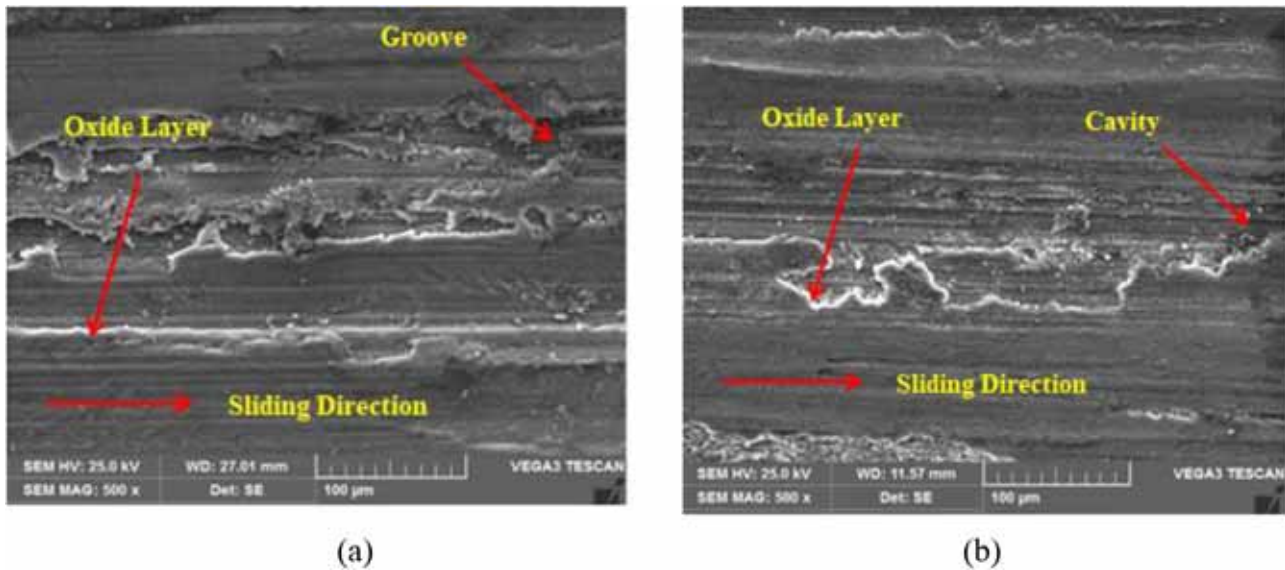


**Fig. 14.** Worn surfaces of (a) As cast Al7075 alloy (b) Al7075-4 % Mica – 5% fly ash-3% Red mud composites.

increases, the co-efficient of friction decreases over a 3000 m sliding distance with a 30 N applied load and 500 rpm sliding speed.

The enhanced wear resistance is due to presence multi particles on the surface are of the wear specimen. These particles make the resistance to plastic deformation at various conditions. The wear loss of Al7075 alloy is more due to soft material as compared to multi particles reinforced composites. The combination of mica, flyash and red mud particles protects the Al matrix from the material loss due to high hardness.

The worn-out surface morphology of Al7075 and its mica, flyash, and red mud particles composites is significant to investigate because it reflects the sort of wear that diverse materials have encountered. During sliding, the Al7075 alloy matrix is smoother than the rubbing disc material, creating viscous flow of aluminium matrix in the shape of a pin, causing plastic deformation of the sample surface and substantial material loss. The worn surface of Al7075 alloy has grooves, micro-pits, and a fractured oxide layer, as shown in Figure 14a, which would have exacerbated wear loss. In Figure 14b, there are fewer cavities and grooves, showing improved wear resistance.

## 4 Conclusions

The Al7075 matrix material with 1 to 5 wt.% of varying flyash, 1 to 3 wt.% of varying red mud and constant 4 wt.% of flyash particles hybrid composites were made-up by stir cast process. The SEM micrographs revealed the presence of redmud, flyash and mica particles in the prepared Al7075 alloy composites. Also, various elements and phases in mica, flyash and red mud particles were identified by EDS and XRD patterns. With the incorporation of these multi reinforcement's hardness and tensile properties of the base

Al7075 alloy matrix was enhanced with decrease in its ductility. Tensile fractured surfaces demonstrated the ductile mode failure in Al7075 alloy and brittle fracture in hybrid composites. Wear resistance of Al7075 alloy was improved with the addition of multi reinforcements with the decrease in co-efficient of friction. Worn surfaces shown more deeper grooves and surface cracks in as cast alloy compared to composites.

## References

1. P.H. Nayak, H.K. Srinivas, M. Nagal, Characterization of tensile fractography of nano ZrO<sub>2</sub> reinforced copper-zinc alloy composites, *Frattura ed Integrità Strutturale (Fracture and Structural Integrity)* **48** (2019) 370–376
2. N. Fazil, V. Venkataramana, M. Nagal, V. Auradi, Synthesis and mechanical characterization of micro B<sub>4</sub>C particulates reinforced AA2124 alloy composites, *Int. J. Eng. Technol. UAE* **7** (2018) 225–229
3. N.G. Siddesh Kumar, G.S. Shivashankar, S. Basavarajappa, R. Suresh, Some studies on mechanical and machining characteristics of Al2219/n-B<sub>4</sub>C/MoS<sub>2</sub> nano hybrid metal matrix composites, *Measurement* **107** (2017) 1–11.
4. G. Pathalinga Prasad, H.C. Chittappa, M. Nagal, V. Auradi, Effect of the reinforcement particle size on the compressive strength and impact toughness of LM29 alloy-B<sub>4</sub>C composites, *Struct. Integr. Life* **19** (2019) 231–236
5. P.R. Jadhav, B.R. Sridhar, M. Nagal, J. Harti, Mechanical behavior and fractography of graphite and boron carbide particulates reinforced A356 alloy hybrid metal matrix composites, *Adv. Compos. Hybrid Mater.* **3** (2020) 114–119
6. C.S. Ramesh, R. Noor Ahmed, M.A. Mujeebu, M.Z. Abdullah, Development and performance analysis of novel cast copper SiC-Gr hybrid composite, *Mater. Des.* **30** (2009) 1957–1965

7. V. Hiremath, S.T. Dundur, R.L. Bharath, G.L. Rajesh, V. Auradi, Studies on mechanical and machinability properties of B<sub>4</sub>C reinforced 6061 aluminium MMC produced via melt stirring, *Appl. Mech. Mater.* **592** (2014) 744–748
8. N. Verma, S.C. Vettivel, Characterization and experimental analysis of boron carbide and rice husk ash reinforced AA7075 aluminium alloy hybrid composites, *J. Alloys Compd.* **741** (2018) 981–998
9. M. Nagaral, V. Auradi, K.I. Parashivamurthy, S.A. Kori, B. K. Shivananda, Synthesis and characterization of Al6061-SiC-graphite composites fabricated by liquid metallurgy, *Mater. Today Proc.* **5** (2018) 2836–2843
10. J. Singh, A. Chuan, Fabrication characteristics and tensile strength of novel Al2024-SiC-red mud composites processing via stir casting route, *Trans. Nonferrous Metals Soc. China* **27** (2017) 2573–2586
11. H. Beygi, S.A. Sajjadi, S.M. Zebarjad, Preparation and characterization of squeeze cast-Al-Si piston alloy reinforced by Ni and nano-Al<sub>2</sub>O<sub>3</sub> particles, *J. King Saud Univ. Eng. Sci.* **28** (2016) 230–239
12. N. Nagaraj, K.V. Mahendra and M. Nagaral, Microstructure and evaluation of mechanical properties of Al-7Si-fly ash composites, *Mater. Today: Proc.* **5** (2018) 3109–3116
13. C. Saravanan, K. Subramanian, V.A. Krishnan, R.S. Narayanan, Effect of particulate reinforced aluminium metal matrix composite – a review, *Mech. Mech. Eng.* **19** (2015) 23–23
14. G.B. Veereshkumar, C.S.P. Rao, N. Selvaraj, Mechanical and tribological behavior of particulate reinforced aluminium metal matrix composites – a review, *J. Minerals Mater. Character. Eng.* **10** (2011) 59–91
15. M. Nagaral, R.G. Deshapande, V. Auradi, S. Babu Boppana, S. Dayanand, M.R. Anilkumar, Mechanical and wear characterization of ceramic boron carbide-reinforced Al2024 alloy metal composites, *J. Bio-and Tribo-Corros.* **7** (2021) 1–12
16. M. Nagaral, V. Auradi, K.I. Parashivamurthy, S.A. Kori, Wear behavior of Al<sub>2</sub>O<sub>3</sub> and graphite particulates reinforced Al6061 alloy hybrid composites, *Am. J. Mater. Sci.* **5** (2015) 25–29
17. M. Nagaral, V. Auradi, S.A. Kori, H.N. Reddappa, Jayachandran, V. Shivaprasad, Studies on 3 and 9 wt.% of B<sub>4</sub>C particulates reinforced Al7025 alloy composites, *AIP Conf. Proc.* **1859** (2019) 020019
18. J. Harti, T.B. Prasad, M. Nagaral, K. Niranjana Rao, Hardness and tensile behavior of Al2219-TiC metal matrix composites, *J. Mech. Eng. Autom.* **6** (2016) 8–12
19. V. Bharath, V. Auradi, M. Nagaral, S. Babu Boppana, Experimental investigations on mechanical and wear behaviour of 2014Al–Al<sub>2</sub>O<sub>3</sub> composites, *J. Bio-and Tribo-Corros.* **6** (2020) 1–10
20. S.N. Prashant, M. Nagaral, V. Auradi, Preparation and evaluation of mechanical and wear properties of Al6061 reinforced with graphite and SiC particulate metal matrix composites, *Int. J. Mech. Eng. Robot. Res.* **1** (2012)

**Cite this article as:** Siddesh Matti, B.P. Shivakumar, Madeva Nagaral, S. Shashidhar, P.N. Siddappa, V. Auradi, Mechanical and tribological behavior of flyash, red mud and mica particles reinforced Al7075 alloy hybrid metal composites, *Manufacturing Rev.* **9**, 11 (2022)